Methoxy aromatic acids in an Arctic ice core from Svalbard: a proxy record of biomass burning

Mackenzie M. Grieman[1], Murat Aydin[1], Elisabeth Isaksson[2], Margit Schwikowski[3], and Eric S. Saltzman[1]

[1]Department of Earth System Science, University of California, Irvine, Irvine, California, 92697-3100, USA
[2]Norwegian Polar Institute Fram Centre NO-9296, Tromsø, Norway
[3]Paul Scherrer Institute, Villigen, Switzerland and Oeschger Centre for Climate Change Research, University of Bern, Switzerland

Correspondence to: Mackenzie M. Grieman (mgrieman@uci.edu)

Abstract. This study presents vanillic acid and para-hydroxybenzoic acid levels in an Arctic ice core from Lomonosovfonna, Svalbard covering the past 800 years. These methoxy aromatic acids are likely derived from lignin combustion in wildfires and long-range aerosol transport. Vanillic and para-hydroxybenzoic acid are present throughout the ice core, confirming that these compounds are preserved on millennial time scales. Vanillic and para-hydroxybenzoic acid concentrations in the Lomonosov-

5 fonna ice core ranged from below the limits of detection to 0.2 and 0.07 ppb, respectively (1 ppb = 1,000 ng/l). Vanillic acid levels are high (below the limit of detection to 0.1 ppb) from 1200-1400 CE, then gradually decline into the 20th century. The largest peak in the vanillic acid in the record occurs from 2000-2008 CE. In the para-hydrobenzoic acid record, there are three centennial-scale peaks around 1300, 1550, and 1650 CE superimposed on a long-term decline in the baseline levels throughout the record. Air mass back trajectory analysis indicates that Siberia and Europe are the primary source regions for

10 wildfire emissions reaching the Lomonosovfonna site. The Lomonosovfonna data are similar to those from the Eurasian Arctic Akademii Nauk ice core during the early part of the record (1220-1400 CE), but the two ice cores diverge markedly after 1400 CE. This coincides with a shift in North Atlantic climate marked by a change of the North Atlantic Oscillation from a positive to a more negative state.

1 Introduction

15 Biomass burning influences the biosphere, atmospheric chemistry, and the climate system on both regional and global scales. Fire influences ecosystem dynamics, ecohydrology, surface albedo, and emissions of chemically and radiatively active aerosols and gases (Crutzen and Andreae, 1990; Legrand et al., 2016; Hessl, 2011; Bowman et al., 2009; Randerson et al., 2006). In boreal regions, fire plays a stabilizing role in circumboreal successional dynamics, influencing boreal forest age structure, species composition, and floristic diversity (Soja et al., 2007). Boreal wildfire areal extent appears to have increased significantly with

20 warming during the past few decades. Boreal forest burned area, fire frequency, fire season length, and fire severity will likely increase with continued warming (Soja et al., 2007; Chapin et al., 2000). Arctic tundra fires are of particular concern because of their potential to release large amounts of ancient permafrost carbon into the atmosphere (Mack et al., 2011).

Understanding the role of fire in the climate system requires a knowledge of past regional/temporal variations and their relationship to climate change on decadal, centennial, and millennial time scales. A number of different types of proxy fire records have been developed but systematic reconstruction of fire history remains a major challenge. Global and regional reconstructions of biomass burning have been developed using sedimentary charcoal records (Marlon et al., 2008, 2016; Power et al., 2008, 2013). The charcoal database is spatially and temporally inhomogeneous, with good coverage in regions of North America and Western Europe, and poor coverage in Asia (accessed at: http://gpwg.paleofire.org; Blarquez et al., 2014). Chemical analyses of inorganic, organic, and particulate constituents in ice core melt water have also been used to reconstruct past variability in biomass burning. These include burning derived markers such as ammonium, organic acids, potassium, and black carbon (see Legrand et al., 2016; Rubino et al., 2015, for recent reviews). Ice core gas measurements of methane and carbon monoxide, and their isotopomers, have also been used to derive histories of pyrogenic emissions (Ferretti et al., 2005; Wang et al., 2010).

Methoxy aromatic acids are among a wide range of phenolic compounds generated by lignin pyrolysis. These compounds are ubiquitous constituents of biomass burning aerosols and have been detected in polar ice cores. Lignin is produced from three precursor alcohols (p-coumaryl alcohol, coniferyl alcohol, and sinapyl alcohol), and the resulting phenolic compounds retain the structure of these alcohols. The aromatic acids analyzed in this study are vanillic acid (VA) and p-hydroxybenzoic acid (p-HBA). VA is predominantly associated with conifer and deciduous boreal forest tree species, while tundra grasses and peat generate primarily p-HBA with lesser amounts of VA (Simoneit, 2002; Oros and Simoneit, 2001a, b; Oros et al., 2006; Iinuma et al., 2007). p-HBA is also produced from conifer boreal tree species (Oros and Simoneit, 2001a).

Burning is the only known source of these methoxy aromatic acids in aerosols or ice cores. Quantitatively, the ice core levels of these compounds result from the combined effects of emissions, atmospheric transport, depositional, and perhaps post-depositional processes. Aromatic acids can undergo re-volatilization at the snow surface. Laboratory experiments have shown that Arctic snow samples containing lignin-derived compounds photochemically react to produce formaldehyde and acetaldehyde (Grannas et al., 2004). Melting and refreezing processes have the potential to redistribute aromatic acids to lower depths. Meltwater at the surface percolates to deeper snow layers and water-soluble compounds are concentrated when the meltwater is refrozen (Wendl et al., 2015).

Prior studies of pyrogenic aromatic acids in ice cores include shallow cores from Greenland, northeast Asia (Kamchatkan Peninsula), and Europe (the Swiss Alps) (McConnell et al., 2007; Kawamura et al., 2012; Müller-Tautges et al., 2016). The record from Greenland showed that the timing of variability in the VA and black carbon records was similar over the past 200 years until around 1890 CE (McConnell et al., 2007). VA and p-HBA were elevated from the 1950's to the 1970's in the 60-year ice core record from the Swiss Alps (Müller-Tautges et al., 2016). VA and p-HBA were elevated in the 1700's and in the 20th century in the ice core from Northeast Asia over the past 300 years. There is only one millennial time scale ice core record of VA and p-HBA: a 2600-year Akademii Nauk ice core record from the Eurasian Arctic (Grieman et al., 2017). That record showed three major multi-century pulses of burning-derived aromatic acids, including one during the Little Ice Age (1450-1700 CE).

Here we present measurements of vanillic acid (VA) and p-hydroxybenzoic acid (p-HBA) in an Arctic ice core from the Lomonosovfonna ice cap in central Spitsbergen, Svalbard, which is located northeast of Greenland, in the Atlantic sector of the Arctic ocean (Fig. 1). The goal of this study was to generate a record sensitive to conditions in Northern Europe/Northern Eurasia. Air mass back trajectories are used to examine the distribution and ecology of likely source regions for biomass

5   burning aerosols transported to Svalbard. We discuss the variability observed in the ice core records of these compounds over the past 750 years, and compare the records to other proxy records of northern hemisphere climate and biomass burning.

2   Methods

2.1   Ice core site characteristics and dating

The Lomonosovfonna ice core site is 1202 m above sea level (asl) (78.82°N, 17.43°E) (Fig. 1). The ice core was drilled in

10   2009 to a depth of 149.5 m by a team from the Paul Scherrer Institute and the Norwegian Polar Institute. The core did not reach bedrock and contains a continuous 750-year record with a basal ice age of 1222 CE (Wendl et al., 2015). The near-surface annual average temperature of Lomonosovfonna is -12.5°C at 1020 m asl (Beaudon et al., 2013; Pohjola et al., 2002; Zagorodnow, 1988). The annual average accumulation rate is 0.58 ± 0.13 m water equivalent (meq) year^{-1} (Wendl et al., 2015). The firn/ice transition occurs at 13 m depth, at approximately 1997 C.E.

15   The Lomonosovfonna ice core was dated by Wendl et al. (2015), yielding a time span for the core of 1222-2009 CE (Fig. S1). Annual layers were counted using seasonal $\delta^{18}O$ and Na^+ variations to a depth of 97.7 m (79.7 m weq), giving an age of 1750 CE at that depth. The chronology of the upper section of the core was also constrained by the ^{210}Pb profile and the 1963 ^3H horizon. The age scale below 97.7 m was developed using a simple glacier ice flow model (Thompson et al., 1998), assuming an average accumulation rate of 0.58 ± 0.13 m weq year^{-1} (Wendl et al., 2015). The age scale was adjusted to

20   match seven volcanic reference horizons. The oldest of these is the Samalas volcanic eruption of 1257/8. Dating uncertainty was estimated by comparing purely modelled reference horizon years to known volcanic eruption years. Above 68 m weq, the dating uncertainty is ± 1 year within 10 years of reference horizons, and ± 3 years otherwise. Between 68-80 m weq, the dating uncertainty is ± 3 years, and below 80 m weq, the dating uncertainty is ± 10 years (Wendl et al., 2015).

The Lomonosovfonna site experiences summer surface melting and winter refreezing (Wendl et al., 2015). Wendl et al.

25   (2015) examined the distribution of melt layers in the Lomonosovfonna ice core, concluding that most summer melt layers are refrozen within the year, with some extending over 2-3 years. The frequency of melt layers increases after 1800 CE (Fig. S2; Wendl et al., 2015). During the warmest years of the twentieth century, percolation length reached 8 years. Due to possible redistribution of soluble compounds by melt, percolation, and refreezing, inter-annual variability of the aromatic acid signals is not interpreted in this study. Ten-year bin averages are used to discuss short-term variability in the data.

2.2 Potential source regions and ecological types using air mass back trajectories

Air mass back trajectories were used to identify potential source regions and ecofloristic zones from which biomass burning aerosols are likely to reach the Lomonosovfonna ice core site. This analysis assumes modern-day meteorological conditions. 10-day air mass back trajectories were computed using the HYSPLIT model with NCEP/NCAR Reanalysis data (Draxler et al.,

5 1999; Stein et al., 2015; Kalnay et al., 1996). The trajectories were started at 100 m above the ice surface at 12:00 AM and 12:00 PM local time for three separate 10-year periods, 1948-1957, 1970-1979, and 2006-2015 CE. The fraction of trajectories originating in or transecting various geographic regions and ecofloristic zones was calculated for spring (March 1-May 31), summer (June 1-Aug. 31), and fall (Sept. 1-Nov. 30). The geographic regions included in the study were North America, Siberia ($>$42°E), and Europe ($<$42°E). These regions were subdivided into ecofloristic zones defined by the Food and Agriculture Or-

10 ganization (FAO; Fig. S3; Ruesch and Gibbs, 2008, http://cdiac.ornl.gov/epubs/ndp/global_carbon/carbon_documentation.html).

The Siberian region has the highest fraction of trajectories to the Lomonosovfonna site, accounting for 39%, 15%, and 38% of the trajectories in spring, summer, and fall from 2006-2015 CE, respectively. Siberian trajectories were most commonly from boreal tundra woodlands, boreal conifer forests, and boreal mountain systems (Fig. S4; Table S1). Fewer than 3% of the trajectories transected other Siberian ecofloristic zones. Europe contributed fewer than 11% of the trajectories arriving at

15 the site in any season. Those trajectories most commonly encountered boreal coniferous forests, boreal mountain systems, and temperate oceanic forests (Fig. S5; Table S1). Pollen species in the Lomonosovfonna ice core covering the past 150 years drilled in 1997 match northern boreal taxa from Fennoscandia (Hicks and Isaksson, 2006). Biomass burning aerosols from Eastern European agricultural fires in 2006 reached Svalbard within a few days (Stohl et al., 2007). Other European ecofloristic zones contributed to fewer than 5% of the trajectories in any season. North America contributed fewer than 4% of the trajectories for

20 any season. This analysis does not rule out contributions from North America, but it does suggest that such input would likely require considerably longer atmospheric transport times.

2.3 Ice core sample preparation and analysis

For this study, we resampled discrete ice core samples previously analyzed for major ions (Wendl et al., 2015). The original ice core samples were 1.8x1.9 cm in cross section and 3-4 cm long, melted and stored frozen in polypropylene vials. For analysis

25 of VA and p-HBA, the ice was re-melted, 1 ml was withdrawn from each vial, and the samples from four adjacent vials were combined into one. This resulted in a total of 997 samples. As discussed below, this sampling procedure resulted in decreasing temporal resolution with increasing depth.

VA and p-HBA in the ice core samples were measured using anion exchange chromatographic separation and tandem mass spectrometric detection in negative ion mode with an electrospray ionization source (IC-ESI-MS/MS). The analytical methods

30 and standards used in this study are described in detail by Grieman et al. (2017). The experimental system consisted of a Dionex AS-AP autosampler, ICS-2100 integrated reagent-free ion chromatograph, and ThermoFinnigan TSQ Quantum triple quadrupole mass spectrometer. VA was detected at two mass transitions (m/z 167→108 and m/z 167→152) and p-HBA was detected at m/z 137→93.

Limits of detection for single measurements were estimated using three times the standard deviation of the MilliQ water blank. The limits of detection for the VA m/z 167→108 and 167→152 transitions were 0.006 and 0.010 ppb (n = 80), respectively. The limit of detection for p-HBA was 0.012 ppb (n = 80). The mass spectrometer signals for VA at the two mass transitions were highly correlated and either mass transition can be used to measure ice core VA (Fig. S6). Data from the m/z

5   167→152 transition is reported here because of the slightly better detection limit.

3   Results and Discussion

3.1   Analytical results and data processing

In this study, 993 samples were analysed for VA and p-HBA (Fig. 2). VA and p-HBA levels range from below detection to 0.2 and 0.07 ppb, respectively. A substantial fraction of the VA and p-HBA data (67% and 58%, respectively) are below

10   detection. Data below the limits of detection are reported as 0.5 times the limit of detection (0.003 ppb for VA and .006 ppb for p-HBA). Smoothing of the data was carried out using both time bin averaging (10, 40, and 100-year) and LOESS smoothing. Both smoothing treatments reveal similar multi-decadal and centennial-scale features in the records and the choice of smoothing technique does not influence the interpretation of the data (Fig. S7). Frequency distributions of the data show skewness towards lower concentrations and geometric means and standard deviations were used in time bin averaging. Time-

15   averaging compensates for the decrease in frequency of sampling with depth in the core due to layer thinning.

3.2   The Lomonosovfonna vanillic and p-hydroxybenzoic acid time series

The Lomonosovfonna VA and p-HBA time series exhibit variability on a wide range of time scales. There is abundant annual to decadal variability in both records. The amplitude of individual peaks in the raw data is roughly similar across the whole record for both compounds, ranging from 0.1-1.2 ppb for VA and 0.1-0.8 for p-HBA (Fig. 2). The peaks appear to be of

20   longer duration during the older portions of both records. Both of these aspects of the raw data are likely artifacts due to the combined effect of annual layer thinning with depth and the sampling strategy of analyzing individual ice core samples of constant thickness (12-16 cm). The time span integrated by individual samples ranged from 1.7 years near the bottom of the core, to 0.5 years at mid-depth (~80 m), to 0.07 years near the top (Fig. S1). This thinning effect is eliminated when the data are time bin-averaged. Peaks in the 10-year bin-averaged records are roughly similar in duration across the whole record (Fig.

25   3). In the bin-averaged data, the magnitudes of the peaks are no longer constant across the record. For VA, the two early peaks (1250-1280 and 1360-1390 CE) are much larger than all subsequent peaks. p-HBA exhibits three major multi-decadal peaks. One is simultaneous with the early VA peak (1250-1280 CE) and the others occur from 1520-1570 and 1610-1640 CE.

Both compounds exhibit long-term decreasing trends over the 800-year record, as illustrated by the 40-year bin averaged data (Fig 3). 40-year bin-averaged VA levels decline by about a factor of three over the first half of the record (1200-1600 CE),

30   then remain relatively steady for the remainder of the record. It is possible that the decline in VA continued after 1600 CE but

much of the data after this time is near or below detection. 40-year bin-averaged p-HBA levels decline by about a factor of two over the whole 800-year record.

Centennial scale variability is observed as pronounced maxima early in the record (1300-1500 CE), as illustrated by the 40-year bin averages (Fig. 3). There are hints of continued centennial scale variability in VA in the remainder of the record.

5 Centennial scale variability is evident throughout the p-HBA record, with maxima coinciding with the VA maxima early on and with additional maxima in the 1500's, 1600's, and 1800's.

The 20th century levels of VA and p-HBA are not anomalous relative to the rest of the ice core record. VA exhibits a slight increase after 1970 and the largest single peak in the record occurs from 2000-2008 CE (Fig. 4). p-HBA levels also appear to increase after 1970, although to a lesser degree than VA. The 2000-2008 period is slightly elevated in p-HBA but not to

10 the extent observed in VA. The samples from 1997-2009 CE are within the firn layer. It is possible that firn samples could be contaminated with biomass burning aerosols during handling in the field but we have no reason to suspect that the methoxy aromatic acids in these samples are influenced by contamination. We have not observed laboratory contamination for these compounds as a significant issue in our laboratory.

Wavelet analysis was used to illustrate temporal variations in the spectral content of the signals. Lomonosovfonna VA and

15 p-HBA time series exhibit non-stationary periodic variability, meaning that the spectral characteristics vary with time (Fig. S8).

3.3   Comparison between Svalbard and Siberian ice core records of vanillic acid and p-hydroxybenzoic acid

The only other millennial scale ice core record of VA and p-HBA is the Akademii Nauk ice core from the Severnaya Zemlya Archipelago in the Arctic Ocean north of central Siberia (Grieman et al., 2017; Fritzsche et al., 2002). The Akademii Nauk ice core covers a considerably larger time range than Lomonsovfonna, extending over the past 2600 years. Here we discuss only

20 the period of temporal overlap between the two ice cores (1200-2000 CE).

The two ice core records exhibit similar trends and levels during the early part of the record (1220-1400 CE; Fig. S9). During this period, Lomonosovfonna exhibits declining levels of both aromatic acids. In the Akademii Nauk core, this period represents the tailing end of an earlier peak in both aromatic acids with a maximum around 1200 CE. The two cores diverge markedly after 1400 CE for the remainder of the records (Fig. 5). Akademii Nauk VA exhibits a period of highly elevated levels

25 from 1460-1660 CE. During this period, Akademii Nauk VA reaches levels more than an order of magnitude above those of Lomonosovfonna VA. Akademii Nauk p-HBA exhibits a period of elevated levels from 1460-1550 and 1780-1860 CE. There are multi-decadal peaks in p-HBA in the Lomonosovfonna record that overlap in time with the large Akademii Nauk VA peaks, although not nearly as large in amplitude or duration. Interestingly, these peaks do not appear at all in the Lomonosovfonna VA record.

30 Back trajectories were computed for the Akademii Nauk site using the same methods as those described above from 2006-2015 CE (section 2.2; Grieman et al., 2017). Both of the Lomonosovfonna and Akademii Nauk sites are influenced by air masses transecting Eurasian forested regions (Fig. 6; Table S1). The highest percentages of trajectories transect Siberian boreal tundra woodland, boreal coniferous forests, and boreal mountain systems for both ice core sites, particularly in the summer and fall. Given this similar transport pattern, we would have expected the two large multi-century peaks in Siberian aromatic acids

after 1400 CE to be exhibited in the Lomonosovfonna record as well. The sharp divergence between the two records around 1400 CE and the subsequent dramatic increase in aromatic acids only in the Siberian ice core suggest a change in transport patterns to the sites after 1400 CE. The fraction of back trajectories transecting vegetated regions of Siberia for Akademii Nauk were about twice that for Lomonosovfonna due to the shorter distance. Conversely, trajectories from European forests comprise

5   a smaller contribution to Akademii Nauk than to Lomonosovfonna. Air masses from European regions are more likely to reach the Lomonsovfonna site than the Akademii Nauk site. We speculate that the divergence between the two ice cores reflects a shift in large-scale atmospheric circulation patterns, as discussed below.

3.4   Relationship to atmospheric circulation and climate

The general climate context for the last millennium is Late Holocene cooling, with superimposed centennial scale climate
10   variability associated with the Medieval Climate Anomaly (MCA, 950-1250 CE), the Little Ice Age (LIA, 1400-1700 CE), and the twentieth century warming (PAGES 2k Consortium, 2013; Lamb, 1965; Mann et al., 2009). Svalbard δ^{18}O ice core records show that cooling continued in the region through the 19th century (Divine et al., 2011). Divine et al. (2011) suggest that the extended LIA at Svalbard could reflect the climatic influence of regional sea ice conditions. In that case, the extended LIA was probably not characteristic of the biomass burning source regions in Europe and Siberia influencing the Lomonosovfonna ice
15   core.

For recent decades, increased burning of wildfires is generally associated with higher summer temperatures (Flannigan et al., 2009). On that basis alone, one might expect to see a long term decrease in aromatic acid signals over the last millennium, and that is generally the case for both VA and p-HBA in the Lomonosovfonna ice core. However, on multi-century and centennial time scales, the variability in the aromatic acids in the Lomonosovfonna ice core is also large and somewhat complex. Both
20   VA and p-HBA levels were high during the MCA. VA declines into the LIA. p-HBA exhibits elevated levels during the latter half of the LIA but VA does not (Fig. 7). This dissimilarity could be due to a shift in the biomass burning source region after 1400 CE.

It seems likely that regional changes in burning proxies on multi-century and centennial time scales are strongly linked to changes in large scale atmospheric circulation and the resulting impacts on regional climate and atmospheric transport. For
25   the source regions influencing the Svalbard Lomonosovfonna ice core, one might expect that changes in the North Atlantic Oscillation (NAO) might play an important role. The NAO is a major mode of climate variability in the North Atlantic region, characterized by changes in the pressure gradient between the Icelandic Low and the Azores High during winter months (Hurrell et al., 2001). Strong pressure gradients (positive NAO index) are associated with strong zonal flow, enhanced westerlies transporting warm air to Europe, increased precipitation in northwest Europe, and decreased precipitation in southern Europe
30   (Trouet et al., 2009). Weaker pressure gradients (negative NAO index) are associated with stronger meridional flow and cooling of the North Atlantic region (Trouet et al., 2012). Proxy NAO records have been developed from variations in wintertime seasalt sodium in the GISP2 ice core, from Moroccan tree-rings and speleothem records in Scotland, and from lake sediments in southwestern Greenland (Meeker and Mayewski, 2002; Trouet et al., 2009; Olsen et al., 2012).

The proxy NAO records show a marked change in phase at the onset of the LIA (around 1400 CE) from several hundred years of positive NAO index to a more negative and variable NAO state that continued throughout and after the LIA (Fig. 7). The Lomonosovfonna oxygen isotope (δ^{18}O) record shows a cooling trend at this time, consistent with the NAO shift (Wendl et al., 2015). The change in NAO behaviour at this time was accompanied by a decline in VA in the Lomonosovfonna record, a

5 decline in the VA/HBA ratio, and a sudden divergence between the Lomonosovfonna and Akademii Nauk ice cores (1400 CE). We propose that a reorganization of high latitude northern hemisphere atmospheric circulation patterns occurred at this time, resulting in 1) a cooler, wetter northern Europe with less burning, and 2) reduced zonal transport, resulting in 'decoupling' of the two ice core signals. Central Siberian burning likely increased at this time, as evidenced by sharply increased aromatic acids in the Akademii Nauk ice core. The Siberian ice core signals are similar in timing to changes in the strength of the Asian

10 monsoon, as recorded in speleothem proxy records (Grieman et al., 2017; Wang et al., 2005). We speculate that during the LIA, central Siberia was influenced primarily by conditions in the Pacific rather than the Atlantic Ocean.

The summertime NAO (SNAO) is defined as the leading mode of July–August sea level pressure variability in the North Atlantic sector (Folland et al., 2009; Efthymiadis et al., 2011). The SNAO affects temperatures, precipitation, and cloudiness in Europe during summer, and one might expect that variations in burning are even more directly linked to the SNAO than the

15 NAO. The SNAO has a slightly different spatial pattern than the NAO, with a relatively small Arctic node and a southern node over northwestern Europe. The positive (negative) mode of the SNAO is characterized by warmer (cooler) summer temperatures over the United Kingdom and lower (higher) precipitation over northern Europe (Linderholm et al., 2008; Folland et al., 2009). The influence of the SNAO extends to central Asia, and so could influence both major source regions for the Lomonosovfonna ice core. Any relationship between SNAO variability and the Lomonosovfonna record could be due to 1) the effect of the

20 SNAO on climate, which in turn affects biomass burning, or 2) changes in atmospheric transport.

SNAO variability has been reconstructed for the past 500 years using historical documents and tree rings (Linderholm et al., 2008, 2009, 2013; Luterbacher et al., 2001). The SNAO record is primarily negative over the past 500 years, with brief positive excursions until the start of the 20th century when it shifted into its positive phase (Linderholm et al., 2009). The long-term trends in the SNAO and NAO reconstructions are generally similar, and there are some common features on centennial time

25 scales (Fig. 7; Trouet et al., 2009). Both NAO and SNAO records exhibit a positive excursion from 1500-1650 CE, during a period of elevated p-HBA in Lomonosovfonna. After 1400 CE, VA remains low and does not show similar timing to p-HBA. This incoherence between the records could be due to the change in atmospheric circulation patterns after 1400 CE when the Svalbard and Siberia ice core records diverge.

In order to explore the possible influence of the SNAO on transport patterns, we compared back trajectories from the

30 Lomonosovfonna site for recent periods when the SNAO index was positive (1970-1979 CE) and negative (1948-1957 CE) (Folland et al., 2009). The average observed SNAO index from 1970-1979 and 1948-1957 CE are 6.3 and -2.0, respectively. Transport from Siberian boreal coniferous forests and mountain systems is slightly higher in the spring and fall and slightly lower in the summer than when the SNAO is negative relative to when it is positive (Fig. 8). Transport from European coniferous forests and mountain systems was slightly higher in the spring, much higher in the summer, and lower in the fall during the

positive phase of the SNAO compared to the negative phase. These results suggest that SNAO-driven variability in atmospheric transport could contribute to variability in burning signals in the Lomonosovfonna record.

3.5 Lomonosovfonna ice core VA/p-HBA ratios

In general, laboratory studies indicate that grasses and trees yield roughly similar emission factors for many organic compounds
5 (i.e. grams emitted per gram of fuel burned). While biomass in forests far exceeds that in grasslands, forest fire recurrence intervals are much longer (van der Werf et al., 2010). Consequently, forests and grasslands make comparable contributions to biomass burning emissions (van der Werf et al., 2010).

Laboratory combustion studies show a wide range in the chemical composition and relative abundance of the various organic compounds generated during biomass burning. Boreal forests in Siberia consist primarily of larch, pine, spruce, and fir tree
10 genera (Soja et al., 2007). We are not aware of laboratory combustion studies using the actual species comprising Siberian boreal forests, but conifers characteristic of North American and European boreal forests have been studied. Lodgepole pine, Sitka spruce, Douglas fir, and Mountain hemlock combustion yielded VA and p-HBA emissions in the range of 1.8-5.9 μg/g conifer fuel burned and VA/p-HBA weight ratios ranging from 0.40-0.99 (Oros and Simoneit, 2001a). Some types of North American conifers produce only one of the two aromatic acids. For example, Eastern White pine produced only VA and Noble
15 fir produced only p-HBA (Oros and Simoneit, 2001a). European pine, European pine with green needles, European spruce with green needles, and peat from western Germany produced VA/p-HBA ratios (μg/g of fuel burned: μg/g of fuel burned) ranging from 0.07-8.75 (14.0:1.6, 0.6:8.1, 2.6:38.0, and 3.0:36.0, respectively; Iinuma et al., 2007). Tundra grass from the Yukon Territories in Canada produced 1.7 μg p-HBA/g fuel burned, but VA was not detected (Oros et al., 2006).

The mean VA/p-HBA ratio for the Lomonosovfonna ice core using the 10-year bin averages of each record is 0.40 $\pm$ 0.25
20 (n=79). The VA/p-HBA ratio is relatively high early in the record, decreasing by a factor of about two from 1200-1500 CE (Fig. 3). The ratio remains low until about 1850 CE, and then increases through the remainder of the record with a sharp increase at 2000 CE. Early in the record, elevated VA/p-HBA ratios are observed in the two major VA spikes around 1270 and 1370 CE. The first VA peak is also a clear peak in p-HBA concentration, but the second VA peak, which is weaker than the first peak, is not evident as a peak in the p-HBA record. From 1540-1620 CE, there is a p-HBA peak without a corresponding peak in the
25 VA record.

The VA/p-HBA ratios observed in the Lomonosovfonna ice core are generally consistent with the laboratory combustion results from boreal forest tree species. Both VA and p-HBA are emitted by the pyrolysis of lignin during the smolering stage of a fire (Akagi et al., 2011; Legrand et al., 2016; Simoneit, 2002). A change in the burning conditions is therefore unlikely to alter the VA/p-HBA ratio. The long-term trends in the VA/p-HBA ratio presumably reflect changes in the relative contributions
30 of fuel types or changes in atmospheric transport. In addition to the long-term trends, there are some notable short-term excursions. It is interesting that these decadal or multi-decadal events all appear as transient increases in the VA/p-HBA ratio and there are no equivalent decreases of similar magnitude. These events are too brief to represent major ecological changes, but too long to represent single events. They could reflect unusual events such as regional prolonged droughts, or multiyear tundra or boreal peat fires. The VA/p-HBA ratio increase after 1800 is likely due to the gradual decrease in the p-HBA baseline.

As noted earlier, the VA baseline appears level after 1800 but is at or near the detection limit. Hence, the apparent change in the VA/p-HBA ratio after 1800 CE may be an artifact of our inability to resolve trends in the very low levels of VA.

3.6 Potential for post depositional modification of VA and p-HBA

There have been no field studies of atmosphere/snow interactions for methoxy aromatic acids like VA and p-HBA, so little is known about postdepositional effects. Three types of effects should be considered: 1) revolatilization after deposition to the snowpack, 2) vertical redistribution associated with melting, percolation, and refreezing, and 3) degradation associated due to chemical or microbiological processes. All three of these effects would likely occur to a greater extent at relatively warm sites like Lomonosovfonna (mean annual temperature -12.5°C) than at cold sites, and during warmer periods like the 20th century, than during the LIA. Redistribution associated with melt layers has been discussed in detail for other ions (Wendl et al., 2015), and one would expect that the influence of these processes on methoxy aromatic acids would be similar. Wendl et al. (2015) used principal component analysis to determine that melt layers did not have a major influence on the distribution of ions on decadal timescales. The VA and p-HBA data from Lomonosovfonna and Akademii Nauk argue against chemical degradation as an important process, since there is clearly no monotonic decrease in VA or p-HBA levels downcore.

The fact that VA and p-HBA are commonly observed in atmospheric aerosols, even after long distance transport, suggests that the volatility of these compounds in aerosols might be considerably lower than that of the pure substance. The vapor pressures for VA and p-HBA are 0.0023 pa and 2.5×10^{-5} pa (https://chem.nlm.nih.gov/chemidplus/rn/121-34-6 Jones, 1960) at 25°C, respectively. Ionic interactions with salts or hydrophobic interactions with soot or complex organics may stabilize aromatic acids in aerosols or snow. Laboratory and aerosol field studies have demonstrated reduced volatility of low molecular weight organic acids (relative to the vapor pressure of the pure compound) due to interaction with cations derived from seasalt or other sources, but this effect has not been studied for aromatic acids (Häkkinen et al., 2014; Laskin et al., 2012).

If re-volatilization of methoxy aromatic acids from the snowpack does occur, one might expect loss be enhanced in ice acidified by high levels of nitrate and sulfate from either volcanic or pollutant inputs. There is no obvious evidence that acidification is a dominant control on VA or p-HBA levels in the ice core (Fig. S10). It is particularly notable that VA and p-HBA levels are not anomalously low during the twentieth century, when ice core sulfate and nitrate levels increased several-fold compared to the preindustrial era (Fig. S10; Fig. S11). Based on the ice core signals alone, we conclude that re-volatilization does not appear to be the predominant factor controlling ice core methoxy aromatic acid levels, although this cannot be ruled out. Further investigation of this issue is needed.

4 Conclusions

The Lomonosovfonna ice core record shows that the methoxy aromatic acids, vanillic acid and para-hydroxybenzoic acid, are present in Arctic ice and preserved on millennial time scales. The observed temporal variability of these signals contains information about the history of high latitude burning in Northern Europe and Siberia. VA and p-HBA are both high from 1200-1400 CE and decline until the Little Ice Age. On centennial timescales, the compounds exhibit some notable differences.

For example, the two largest peaks in the p-HBA record around 1600 CE are not part of the VA record. This difference in the records could be due to a change in the vegetation type burned or atmospheric transport pattern to the ice core site. The highest levels of VA exhibited from 2000-2008 CE are not shown in the p-HBA record. Further studies of VA levels in snow pits near the ice core site should be conducted to confirm these recent high levels of VA. It should be noted that these records

5 have not been validated or calibrated by comparison to instrumental or satellite trends in biomass burning. Shallow ice core measurements of these compounds covering over the instrumental period across the Arctic are needed.

The two millennial scale ice cores analysed for these compounds to date, Lomonosovfonna and Akademii Nauk, show intriguing similarity between the Svalbard and Siberian records at the end of the Medieval Climate Anomaly (1200-1400 CE) but dramatic differences for most of the past millennium. Such differences are surprising given that air mass trajectories based

10 on reanalysis data indicate considerable overlap in source areas for the two ice cores. It seems that there must exist a large-scale dynamical explanation of the regional/temporal trends in these and other proxy fire records. Developing a unified interpretation of these signals will require further work.

5   Data availability

The data reported in this manuscript will be submitted to the NSF Artic Data Center (http://arcticdata.io/) before publication.

15 *Author contributions.* Mackenzie Grieman, Murat Aydin, and Eric Saltzman developed the analytical method. Mackenzie Grieman combined and measured the ice core melt samples used in this study and processed the data. Mackenzie Grieman and Eric Saltzman wrote the manuscript. Margit Schwikowski and her team drilled and processed the ice core, provided samples, developed the depth-age scale, and provided comments on the manuscript. Elisabeth Isaksson initiated the Lomonosovfonna ice core drilling project, was responsible for field logistics, and provided comments on the manuscript. Murat Aydin provided comments on the manuscript.

20 *Competing interests.* The authors declare that they have no conflicts of interest.

References

Akagi, S. K., Yokelson, R. J., Wiedinmyer, C., Alvarado, M. J., Reid, J. S., Karl, T., Crounse, J. D., and Wennberg, P. O.: Emission factors for open and domestic biomass burning for use in atmospheric models, Atmospheric Chemistry and Physics, 11, 4039–4072, doi:10.5194/acp-11-4039-2011, 2011.

5 Beaudon, E., Moore, J. C., Martma, T., Pohjola, V. A., Van De Wal, R. S., Kohler, J., and Isaksson, E.: Lomonosovfonna and Holtedahl-fonna ice cores reveal eastwest disparities of the Spitsbergen environment since AD 1700, Journal of Glaciology, 59, 1069–1083, doi:doi:10.3189/2013JoG12J203, 2013.

Blarquez, O., Vannière, B., Marlon, J. R., Daniau, A.-L., Power, M. J., Brewer, S., and Bartlein, P. J.: Paleofire: An R package to analyse sedimentary charcoal records from the Global Charcoal Database to reconstruct past biomass burning, Computers and Geosciences, 72,

10 255 – 261, doi:10.1016/j.cageo.2014.07.020, 2014.

Bowman, D. M., Balch, J. K., Artaxo, P., Bond, W. J., Carlson, J. M., Cochrane, M. A., D'Antonio, C. M., DeFries, R. S., Doyle, J. C., Harrison, S. P., et al.: Fire in the Earth system, science, 324, 481–484, doi:10.1126/science.1163886, 2009.

Chapin, F. S., Mcguire, A. D., Randerson, J., Pielke, R., Baldocchi, D., Hobbie, S. E., Roulet, N., Eugster, W., Kasischke, E., Rastetter, E. B., Zimov, S. A., and Running, S. W.: Arctic and boreal ecosystems of western North America as components of the climate system, Global

15 Change Biology, 6, 211–223, doi:10.1046/j.1365-2486.2000.06022.x, 2000.

Crutzen, P. J. and Andreae, M. O.: Biomass Burning in the Tropics: Impact on Atmospheric Chemistry and Biogeochemical Cycles, Science, 250, 1669–1678, doi:10.1126/science.250.4988.1669, 1990.

Divine, D., Isaksson, E., Martma, T., Meijer, H. A., Moore, J., Pohjola, V., van de Wal, R. S. W., and Godtliebsen, F.: Thousand years of winter surface air temperature variations in Svalbard and northern Norway reconstructed from ice-core data, Polar Research, 30, 7379,

20 doi:10.3402/polar.v30i0.7379, 2011.

Draxler, R. R., Stunder, B., Rolph, G., and Taylor, A.: HYSPLIT4 user's guide, NOAA Technical Memorandum ERL ARL, 230, 35, 1999.

Efthymiadis, D., Goodess, C., and Jones, P.: Trends in Mediterranean gridded temperature extremes and large-scale circulation influences, Natural Hazards and Earth System Sciences, 11, 2199, doi:10.5194/nhess-11-2199-2011, 2011.

Ferretti, D. F., Miller, J. B., White, J. W. C., Etheridge, D. M., Lassey, K. R., Lowe, D. C., Meure, C. M. M., Dreier, M. F., Trudinger, C. M.,

25 van Ommen, T. D., and Langenfelds, R. L.: Unexpected Changes to the Global Methane Budget over the Past 2000 Years, Science, 309, 1714–1717, doi:10.1126/science.1115193, 2005.

Flannigan, M. D., Krawchuk, M. A., de Groot, W. J., Wotton, B. M., and Gowman, L. M.: Implications of changing climate for global wildland fire, International journal of wildland fire, 18, 483–507, doi:10.1071/WF08187, 2009.

Folland, C. K., Knight, J., Linderholm, H. W., Fereday, D., Ineson, S., and Hurrell, J. W.: The summer North Atlantic Oscillation: past,

30 present, and future, Journal of Climate, 22, 1082–1103, doi:10.1175/2008JCLI2459.1, 2009.

Fritzsche, D., Wilhelms, F., Savatyugin, L. M., Pinglot, J. F., Meyer, H., Hubberten, H.-W., and Miller, H.: A new deep ice core from Akademii Nauk ice cap, Severnaya Zemlya, Eurasian Arctic: first results, Annals of Glaciology, 35, 25–28, doi:10.3189/172756402781816645, 2002.

Grannas, A. M., Shepson, P. B., and Filley, T. R.: Photochemistry and nature of organic matter in Arctic and Antarctic snow, Global Bio-geochem. Cycles, 18, GB1006, doi:10.1029/2003GB002133, 2004.

35 Grieman, M. M., Aydin, M., Fritzsche, D., McConnell, J. R., Opel, T., Sigl, M., and Saltzman, E. S.: Aromatic acids in a Eurasian Arctic ice core: a 2600-year proxy record of biomass burning, Climate of the Past, 13, 395–410, doi:10.5194/cp-13-395-2017, 2017.

Hessl, A. E.: Pathways for climate change effects on fire: Models, data, and uncertainties, Progress in Physical Geography, 35, 393–407, doi:10.1177/0309133311407654, 2011.

Hicks, S. and Isaksson, E.: Assessing source areas of pollutants from studies of fly ash, charcoal, and pollen from Svalbard snow and ice, Journal of Geophysical Research: Atmospheres, 111, doi:10.1029/2005JD006167, 2006.

Häkkinen, S. A. K., McNeill, V. F., and Riipinen, I.: Effect of Inorganic Salts on the Volatility of Organic Acids, Environmental Science & Technology, 48, 13 718–13 726, doi:10.1021/es5033103, 2014.

Hunter, J. D.: Matplotlib: A 2D Graphics Environment, Computing in Science & Engineering, 9, 90–95, doi:10.1109/MCSE.2007.55, 2007.

Hurrell, J. W., Kushnir, Y., and Visbeck, M.: The North Atlantic Oscillation, Science, 291, 603–605, doi:10.1126/science.1058761, 2001.

Iinuma, Y., Brüggemann, E., Gnauk, T., Müller, K., Andreae, M. O., Helas, G., Parmar, R., and Herrmann, H.: Source characterization of biomass burning particles: The combustion of selected European conifers, African hardwood, savanna grass, and German and Indonesian peat, Journal of Geophysical Research: Atmospheres, 112, D08 209, doi:10.1029/2006JD007120, 2007.

Jones, A. H.: Sublimation Pressure Data for Organic Compounds., Journal of Chemical and Engineering Data, 5, 196–200, 1960.

Kalnay, E., Kanamitsu, M., Kistler, R., Collins, W., Deaven, D., Gandin, L., Iredell, M., Saha, S., White, G., Woollen, J., Zhu, Y., Leetmaa, A., Reynolds, B., Chelliah, M., Ebisuzaki, W., Higgins, W., Janowiak, J., Mo, K., Ropelewski, C., Wang, J., Jenne, R., and Joseph, D.: The NCEP/NCAR 40-Year Reanalysis Project, Bulletin of the American Meteorological Society, 77, 437–471, 1996.

Kawamura, K., Izawa, Y., Mochida, M., and Shiraiwa, T.: Ice core records of biomass burning tracers (levoglucosan and dehydroabietic, vanillic and p-hydroxybenzoic acids) and total organic carbon for past 300 years in the Kamchatka Peninsula, Northeast Asia, Geochimica et Cosmochimica Acta, 99, doi:10.1016/j.gca.2012.08.006, 2012.

Lamb, H.: The early medieval warm epoch and its sequel, Palaeogeography, Palaeoclimatology, Palaeoecology, 1, 13–37, doi:10.1016/0031-0182(65)90004-0, 1965.

Laskin, A., Moffet, R. C., Gilles, M. K., Fast, J. D., Zaveri, R. A., Wang, B., Nigge, P., and Shutthanandan, J.: Tropospheric chemistry of internally mixed sea salt and organic particles: Surprising reactivity of NaCl with weak organic acids, Journal of Geophysical Research: Atmospheres, 117, D15 302, doi:10.1029/2012JD017743, 2012.

Legrand, M., McConnell, J., Fischer, H., Wolff, E. W., Preunkert, S., Arienzo, M., Chellman, N., Leuenberger, D., Maselli, O., Place, P., Sigl, M., Schüpbach, S., and Flannigan, M.: Boreal fire records in Northern Hemisphere ice cores: a review, Climate of the Past, 12, 2033–2059, doi:10.5194/cp-12-2033-2016, 2016.

Linderholm, H., Folland, C., and Hurrell, J.: Reconstructing Summer North Atlantic Oscillation (SNAO) variability over the last five centuries, Tree rings in archaeology. Clim Ecol, 6, 8–16, doi:10.2312/GFZ.b103-08056, 2008.

Linderholm, H. W., Folland, C. K., and Walther, A.: A multicentury perspective on the summer North Atlantic Oscillation (SNAO) and drought in the eastern Atlantic Region, Journal of Quaternary Science, 24, 415–425, doi:10.1002/jqs.1261, 2009.

Linderholm, H. W., Seim, A., Ou, T., Jeong, J.-H., Liu, Y., Wang, X., Bao, G., and Folland, C.: Exploring teleconnections between the summer {NAO} (SNAO) and climate in East Asia over the last four centuries – A tree-ring perspective, Dendrochronologia, 31, 297 – 310, doi:10.1016/j.dendro.2012.08.004, 2013.

Luterbacher, J., Xoplaki, E., Dietrich, D., Jones, P. D., Davies, T. D., Portis, D., Gonzalez-Rouco, J. F., von Storch, H., Gyalistras, D., Casty, C., and Wanner, H.: Extending North Atlantic oscillation reconstructions back to 1500, Atmospheric Science Letters, 2, 114–124, doi:10.1006/asle.2002.0047, http://dx.doi.org/10.1006/asle.2002.0047, 2001.

Mack, M. C., Bret-Harte, M. S., Hollingsworth, T. N., Jandt, R. R., Schuur, E. A. G., Shaver, G. R., and Verbyla, D. L.: Carbon loss from an unprecedented Arctic tundra wildfire, Nature, 475, 489–492, doi:10.1038/nature10283, 2011.

Mann, M. E., Zhang, Z., Rutherford, S., Bradley, R. S., Hughes, M. K., Shindell, D., Ammann, C., Faluvegi, G., and Ni, F.: Global Signatures and Dynamical Origins of the Little Ice Age and Medieval Climate Anomaly, Science, 326, 1256–1260, doi:10.1126/science.1177303, 2009.

Marlon, J. R., Bartlein, P. J., Carcaillet, C., Gavin, D. G., Harrison, S. P., Higuera, P. E., Joos, F., Power, M. J., and Prentice, I. C.: Climate
5   and human influences on global biomass burning over the past two millennia, Nature Geosci, 1, 697–702, doi:10.1038/ngeo313, 2008.

Marlon, J. R., Kelly, R., Daniau, A.-L., Vannière, B., Power, M. J., Bartlein, P., Higuera, P., Blarquez, O., Brewer, S., Brücher, T., Feurdean,
    A., Romera, G. G., Iglesias, V., Maezumi, S. Y., Magi, B., Courtney Mustaphi, C. J., and Zhihai, T.: Reconstructions of biomass burning
    from sediment-charcoal records to improve data–model comparisons, Biogeosciences, 13, 3225–3244, doi:10.5194/bg-13-3225-2016,
    2016.

10   Mayewski, P. A., Meeker, L. D., Twickler, M. S., Whitlow, S., Yang, Q., Lyons, W. B., and Prentice, M.: Major features and forcing of high-
    latitude northern hemisphere atmospheric circulation using a 110,000-year-long glaciochemical series, Journal of Geophysical Research:
    Oceans, 102, 26 345–26 366, doi:10.1029/96JC03365, 1997.

McConnell, J. R., Edwards, R., Kok, G. L., Flanner, M. G., Zender, C. S., Saltzman, E. S., Banta, J. R., Pasteris, D. R., Carter, M. M.,
    and Kahl, J. D. W.: 20th-Century Industrial Black Carbon Emissions Altered Arctic Climate Forcing, Science, 317, 1381–1384,
15   doi:10.1126/science.1144856, 2007.

Meeker, L. D. and Mayewski, P. A.: A 1400-year high-resolution record of atmospheric circulation over the North Atlantic and Asia, The
    Holocene, 12, 257–266, doi:10.1191/0959683602hl542ft, 2002.

Müller-Tautges, C., Eichler, A., Schwikowski, M., Pezzatti, G. B., Conedera, M., and Hoffmann, T.: Historic records of organic compounds
    from a high Alpine glacier: influences of biomass burning, anthropogenic emissions, and dust transport, Atmospheric Chemistry and
20   Physics, 16, 1029–1043, doi:10.5194/acp-16-1029-2016, 2016.

Olsen, J., Anderson, N. J., and Knudsen, M. F.: Variability of the North Atlantic Oscillation over the past 5,200 years, Nature Geoscience, 5,
    808–812, 2012.

Oros, D. R. and Simoneit, B. R. T.: Identification and emission factors of molecular tracers in organic aerosols from biomass burning Part 1.
    Temperate climate conifers, Applied Geochemistry, 16, 1513–1544, doi:10.1016/s0883-2927(01)00021-x, 2001a.

25   Oros, D. R. and Simoneit, B. R. T.: Identification and emission factors of molecular tracers in organic aerosols from biomass burning Part 2.
    Deciduous trees, Applied Geochemistry, 16, 1545–1565, doi:10.1016/S0883-2927(01)00022-1, 2001b.

Oros, D. R., Abas, M. R. b., Omar, N. Y. M. J., Rahman, N. A., and Simoneit, B. R. T.: Identification and emission factors of molecular tracers
    in organic aerosols from biomass burning: Part 3. Grasses, Applied Geochemistry, 21, 919–940, doi:10.1016/j.apgeochem.2006.01.008,
    2006.

30   PAGES 2k Consortium, .: Continental-scale temperature variability during the past two millennia, Nature Geoscience, 6, 339–346,
    doi:10.1038/ngeo1797, 2013.

Pohjola, V. A., Moore, J. C., Isaksson, E., Jauhiainen, T., van de Wal, R. S. W., Martma, T., Meijer, H. A. J., and Vaikmäe, R.: Effect of
    periodic melting on geochemical and isotopic signals in an ice core from Lomonosovfonna, Svalbard, Journal of Geophysical Research:
    Atmospheres, 107, ACL 1–1–ACL 1–14, doi:10.1029/2000JD000149, 2002.

35   Power, M., Marlon, J., Ortiz, N., Bartlein, P., Harrison, S., Mayle, F., Ballouche, A., Bradshaw, R., Carcaillet, C., Cordova, C., Mooney, S.,
    Moreno, P., Prentice, I., Thonicke, K., Tinner, W., Whitlock, C., Zhang, Y., Zhao, Y., Ali, A., Anderson, R., Beer, R., Behling, H., Briles,
    C., Brown, K., Brunelle, A., Bush, M., Camill, P., Chu, G., Clark, J., Colombaroli, D., Connor, S., Daniau, A. L., Daniels, M., Dodson, J.,
    Doughty, E., Edwards, M., Finsinger, W., Foster, D., Frechette, J., Gaillard, M. J., Gavin, D., Gobet, E., Haberle, S., Hallett, D., Higuera, P.,

Hope, G., Horn, S., Inoue, J., Kaltenrieder, P., Kennedy, L., Kong, Z., Larsen, C., Long, C., Lynch, J., Lynch, E., McGlone, M., Meeks, S., Mensing, S., Meyer, G., Minckley, T., Mohr, J., Nelson, D., New, J., Newnham, R., Noti, R., Oswald, W., Pierce, J., Richard, P., Rowe, C., Sanchez Goñi, M., Shuman, B., Takahara, H., Toney, J., Turney, C., Urrego-Sanchez, D., Umbanhowar, C., Vandergoes, M., Vanniere, B., Vescovi, E., Walsh, M., Wang, X., Williams, N., Wilmshurst, J., and Zhang, J.: Changes in fire regimes since the Last Glacial Maximum: an assessment based on a global synthesis and analysis of charcoal data, Climate Dynamics, 30, 887–907, doi:10.1007/s00382-007-0334-x, 2008.

Power, M., Mayle, F., Bartlein, P., Marlon, J., Anderson, R., Behling, H., Brown, K., Carcaillet, C., Colombaroli, D., Gavin, D., Hallett, D., Horn, S., Kennedy, L., Lane, C., Long, C., Moreno, P., Paitre, C., Robinson, G., Taylor, Z., and Walsh, M.: Climatic control of the biomass-burning decline in the Americas after AD 1500, The Holocene, 23, 3–13, doi:10.1177/0959683612450196, 2013.

Randerson, J. T., Liu, H., Flanner, M. G., Chambers, S. D., Jin, Y., Hess, P. G., Pfister, G., Mack, M. C., Treseder, K. K., Welp, L. R., Chapin, F. S., Harden, J. W., Goulden, M. L., Lyons, E., Neff, J. C., Schuur, E. A. G., and Zender, C. S.: The Impact of Boreal Forest Fire on Climate Warming, Science, 314, 1130–1132, 10.1126/science.1132075, 2006.

Rubino, M., D'Onofrio, A., Seki, O., and Bendle, J. A.: Ice-core records of biomass burning, The Anthropocene Review, p. 2053019615605117, doi:10.1177/2053019615605117, 2015.

Ruesch, A. and Gibbs, H. K.: New IPCC Tier-1 global biomass carbon map for the year 2000, Carbon Dioxide Information Analysis Center, Oak Ridge National Laboratory, 2008.

Simoneit, B. R. T.: Biomass burning - A review of organic tracers for smoke from incomplete combustion, Applied Geochemistry, 17, 129–162, doi:10.1016/S0883-2927(01)00061-0, 2002.

Soja, A. J., Tchebakova, N. M., French, N. H., Flannigan, M. D., Shugart, H. H., Stocks, B. J., Sukhinin, A. I., Parfenova, E., III, F. S. C., and Jr., P. W. S.: Climate-induced boreal forest change: Predictions versus current observations, Global and Planetary Change, 56, 274 – 296, doi:http://dx.doi.org/10.1016/j.gloplacha.2006.07.028, 2007.

Stein, A., Draxler, R., Rolph, G., Stunder, B., Cohen, M., and Ngan, F.: NOAA's HYSPLIT atmospheric transport and dispersion modeling system, Bulletin of the American Meteorological Society, 96, 2059–2077, doi:10.1175/BAMS-D-14-00110.1, 2015.

Stohl, A., Berg, T., Burkhart, J., Fjæraa, A., Forster, C., Herber, A., Hov, Ø., Lunder, C., McMillan, W., Oltmans, S., Shiobara, M., Simpson, D., Solberg, S., Stebel, K., Ström, J., Tørseth, K., Treffeisen, R., Virkkunen, K., and Yttri, K. E.: Arctic smoke–record high air pollution levels in the European Arctic due to agricultural fires in Eastern Europe in spring 2006, Atmospheric Chemistry and Physics, 7, 511–534, doi:10.5194/acp-7-511-2007, 2007.

Thompson, L. G., Davis, M. E., Mosley-Thompson, E., Sowers, T. A., Henderson, K. A., Zagorodnov, V. S., Lin, P.-N., Mikhalenko, V. N., Campen, R. K., Bolzan, J. F., Cole-Dai, J., and Francou, B.: A 25,000-Year Tropical Climate History from Bolivian Ice Cores, Science, 282, 1858–1864, doi:10.1126/science.282.5395.1858, 1998.

Torrence, C. and Compo, G. P.: A practical guide to wavelet analysis, Bulletin of the American Meteorological society, 79, 61–78, doi:10.1175/1520-0477(1998)079<0061:APGTWA>2.0.CO;2, 1998.

Trouet, V., Esper, J., Graham, N. E., Baker, A., Scourse, J. D., and Frank, D. C.: Persistent Positive North Atlantic Oscillation Mode Dominated the Medieval Climate Anomaly, Science, 324, 78–80, doi:10.1126/science.1166349, 2009.

Trouet, V., Scourse, J., and Raible, C.: North Atlantic storminess and Atlantic Meridional Overturning Circulation during the last Millennium: Reconciling contradictory proxy records of NAO variability, Global and Planetary Change, 84–85, 48–55, doi:10.1016/j.gloplacha.2011.10.003, 2012.

van der Werf, G. R., Randerson, J. T., Giglio, L., Collatz, G. J., Mu, M., Kasibhatla, P. S., Morton, D. C., DeFries, R. S., Jin, Y., and van Leeuwen, T. T.: Global fire emissions and the contribution of deforestation, savanna, forest, agricultural, and peat fires (1997–2009), Atmospheric Chemistry and Physics, 10, 11 707–11 735, doi:10.5194/acp-10-11707-2010, 2010.

Wang, Y., Cheng, H., Edwards, R. L., He, Y., Kong, X., An, Z., Wu, J., Kelly, M. J., Dykoski, C. A., and Li, X.: The Holocene Asian
5   Monsoon: Links to Solar Changes and North Atlantic Climate, Science, 308, 854–857, doi:10.1126/science.1106296, 2005.

Wang, Z., Chappellaz, J., Park, K., and Mak, J.: Large variations in Southern Hemisphere biomass burning during the last 650 years, Science, 330, 1663–1666, doi:10.1126/science.1197257, 2010.

Wendl, I., Eichler, A., Isaksson, E., Martma, T., and Schwikowski, M.: 800-year ice-core record of nitrogen deposition in Svalbard linked to ocean productivity and biogenic emissions, Atmospheric Chemistry and Physics, 15, 7287–7300, 2015.

10   Zagorodnow, V. S.: Recent Soviet activities on ice core drilling and core investigations in Arctic region, Bull. Glacier Res., p. 81–84, 1988.
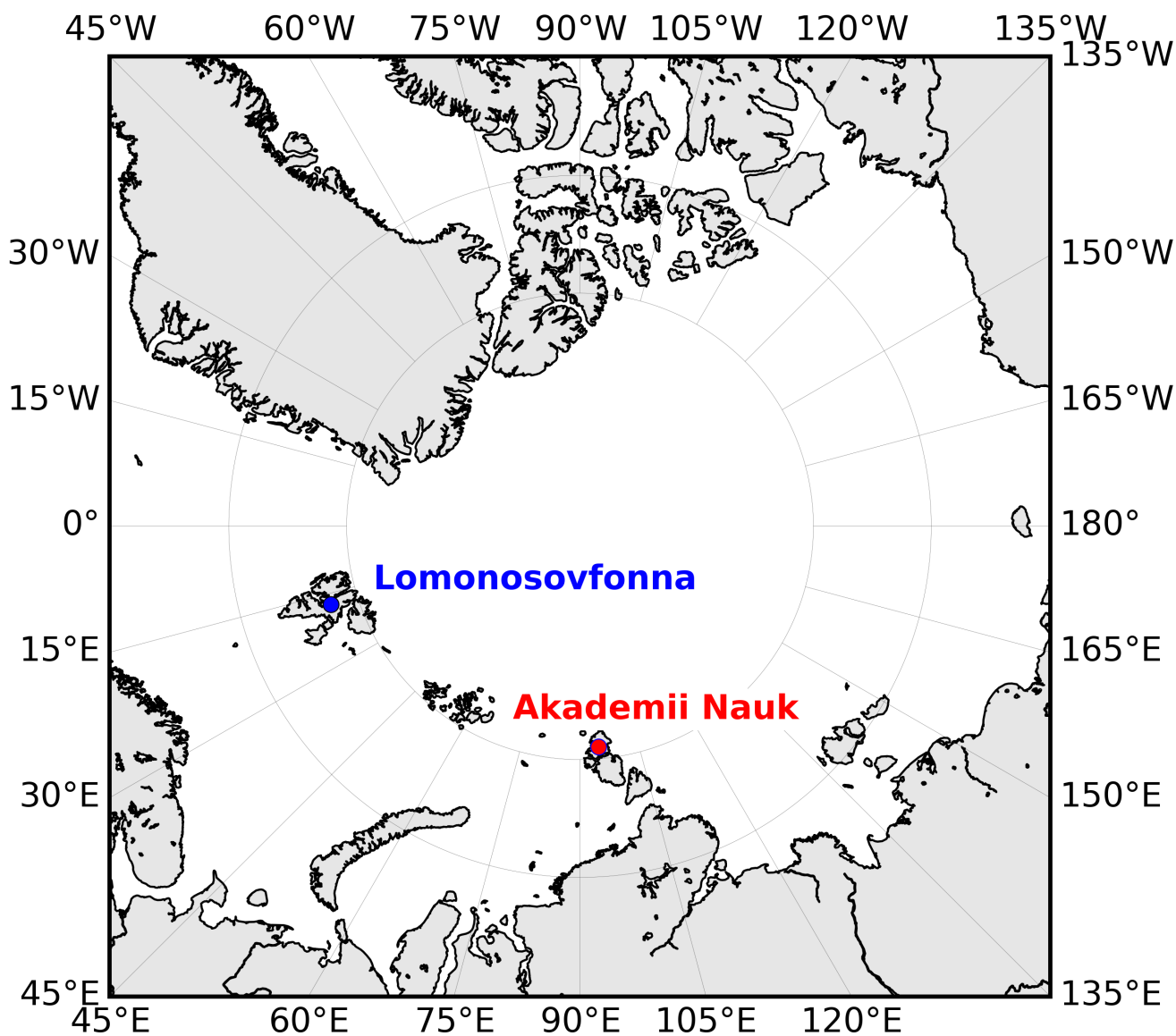
Figure 1. Location of Lomonosovfonna ice core drilling site on the island of Spitsbergen in Svalbard (78°49'24.4"N, 17°25'59.2"E) and the Akademii Nauk ice core drilling site on Severnaya Zemlya (80°31'N, 94°49'E). The map was produced in the Python "matplotlib" graphics environment (Hunter, 2007).
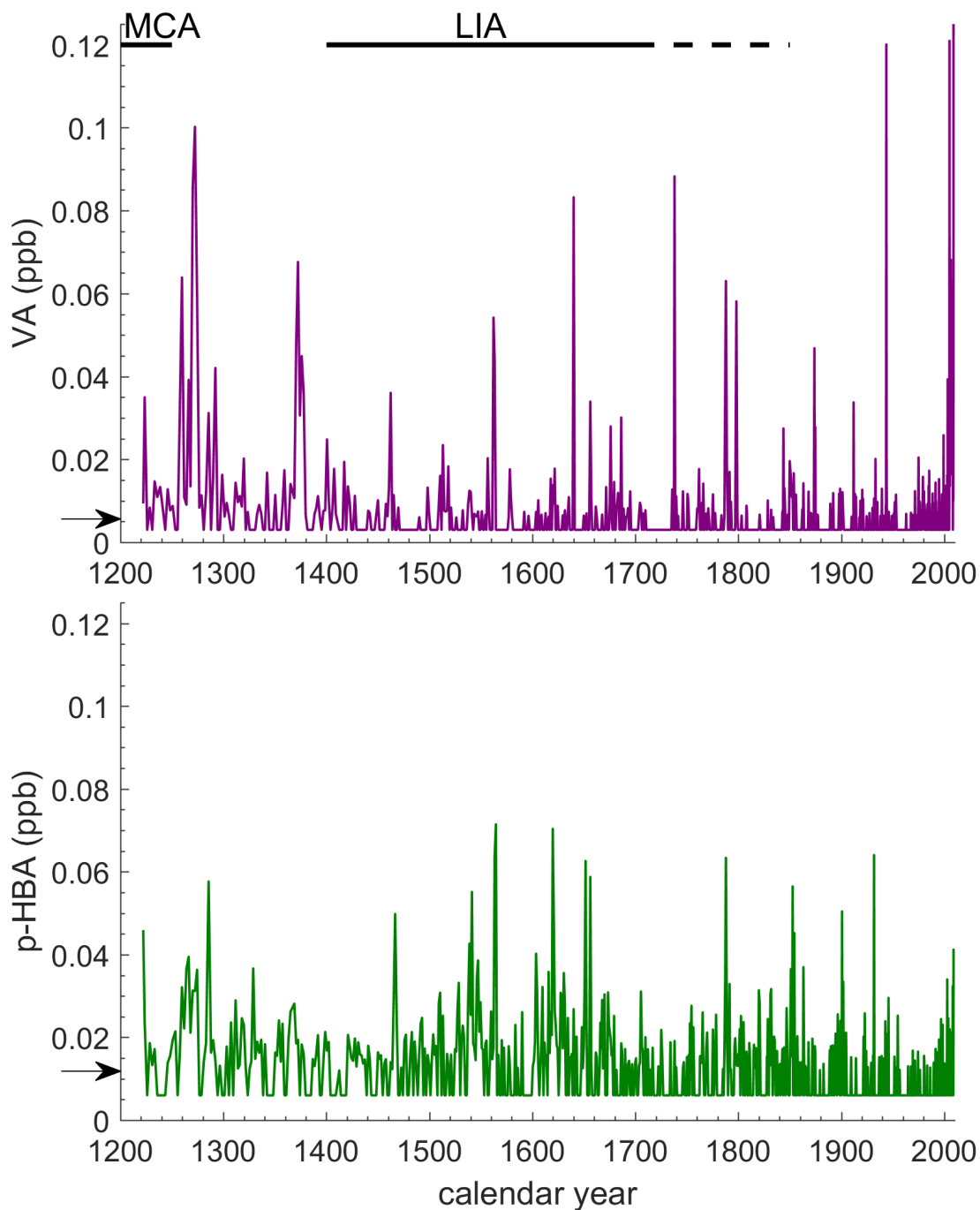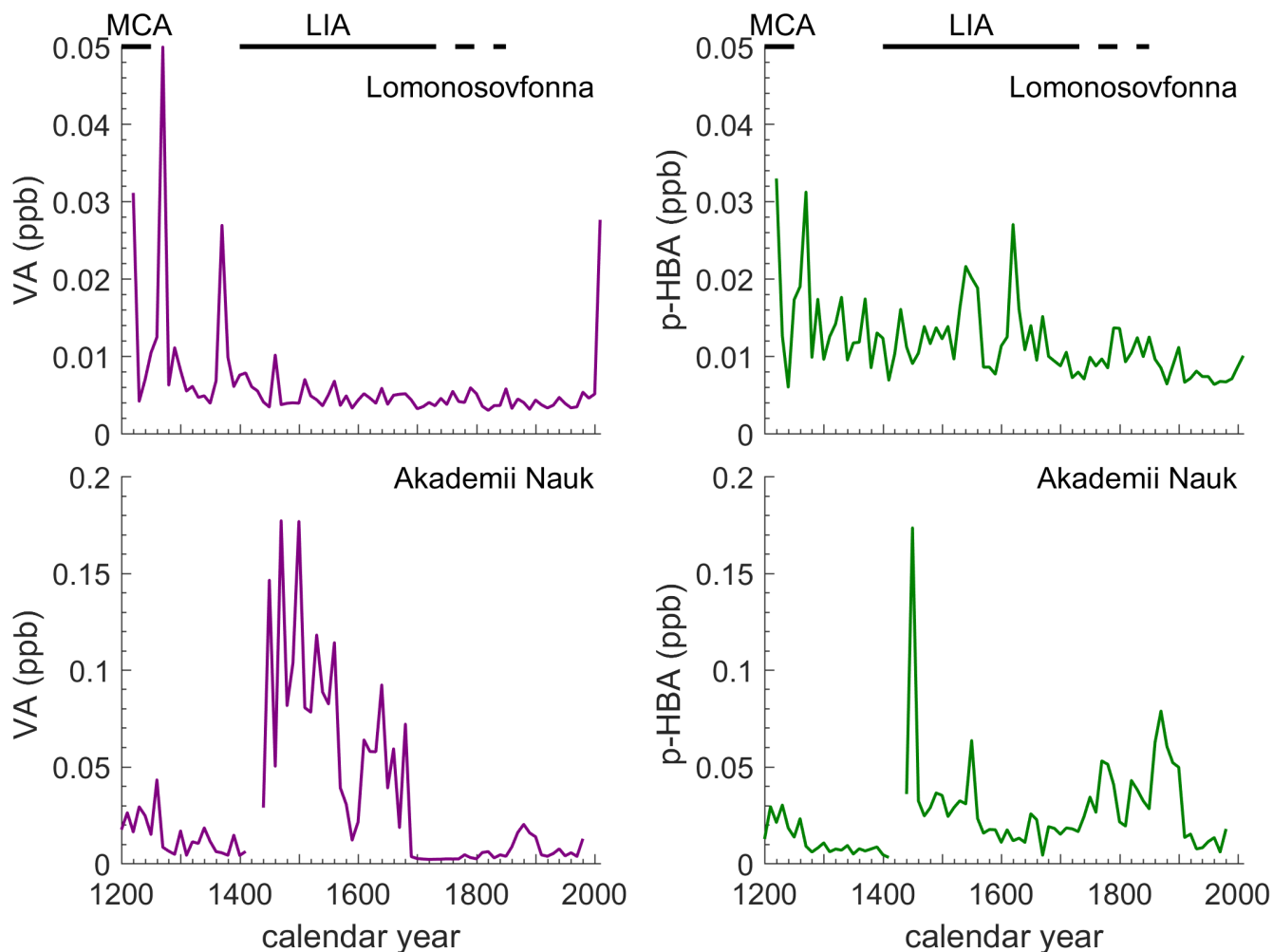
Figure 2. Aromatic acids in the Lomonosovfonna, Svalbard ice core. Top: vanillic acid, Bottom: p-hydroxybenzoic acid. Arrows are the detection limits. The black horizontal lines are the Medieval Climate Anomaly (MCA) and the Little Ice Age (LIA) (Mann et al., 2009). The dashed horizontal line is the extended LIA in the Svalbard region (Divine et al., 2011).

Climate
of the Past
Discussions
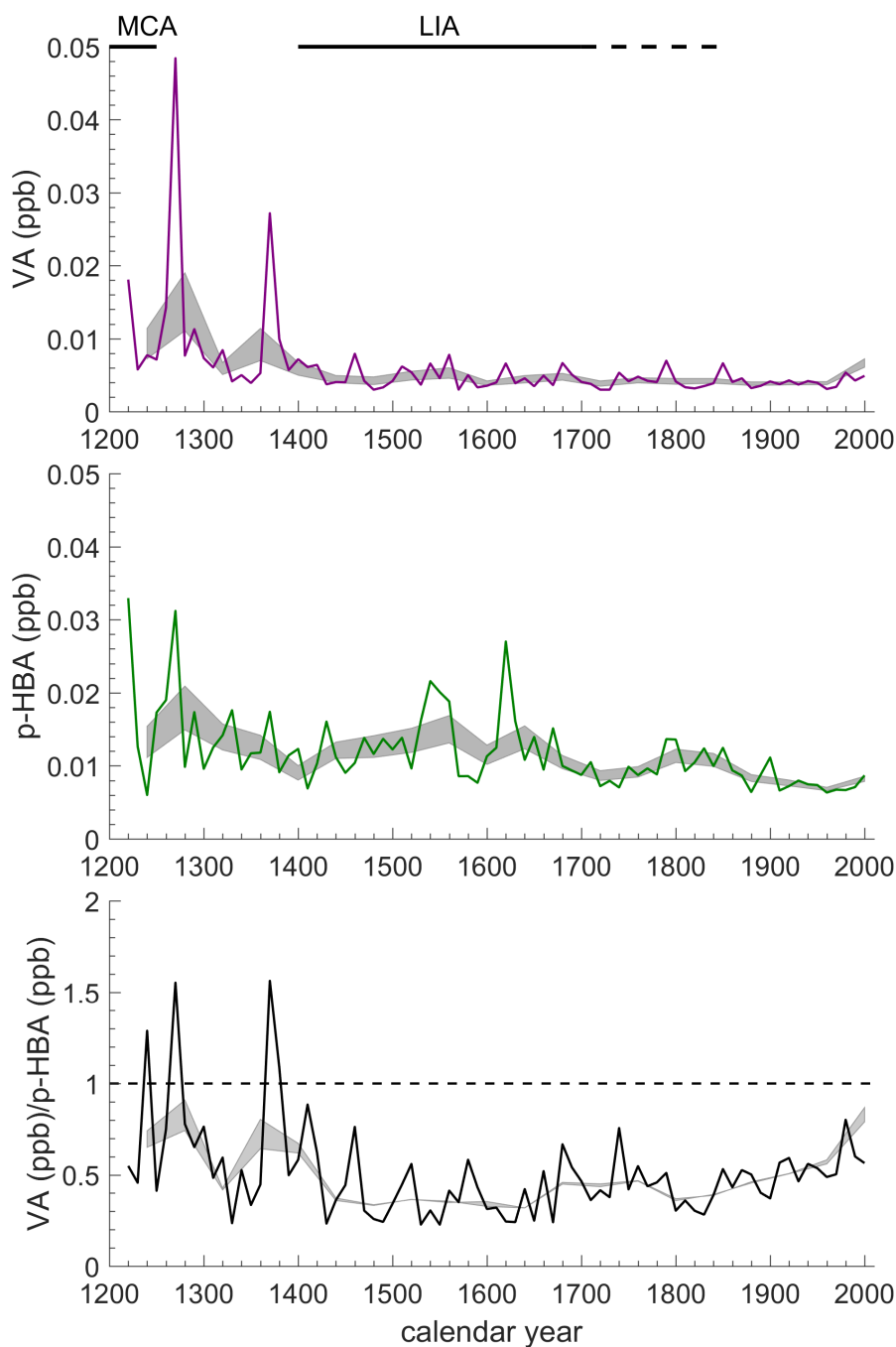
Figure 3. Lomonosovfonna ice core records of vanillic acid (top) and p-hydroxybenzoic acid (middle) and the ratio of vanillic acid/p-hydroxybenzoic acid (bottom). For all plots: black lines are 10-year bin averages, gray shaded areas are 40-year bin averages of ±1 standard error. The dashed line on the bottom plot indicates a ratio of 1. The black horizontal lines are the Medieval Climate Anomaly (MCA) and the Little Ice Age (LIA) (Mann et al., 2009). The dashed horizontal line at the top is the extended LIA in the Svalbard region (Divine et al., 2011).
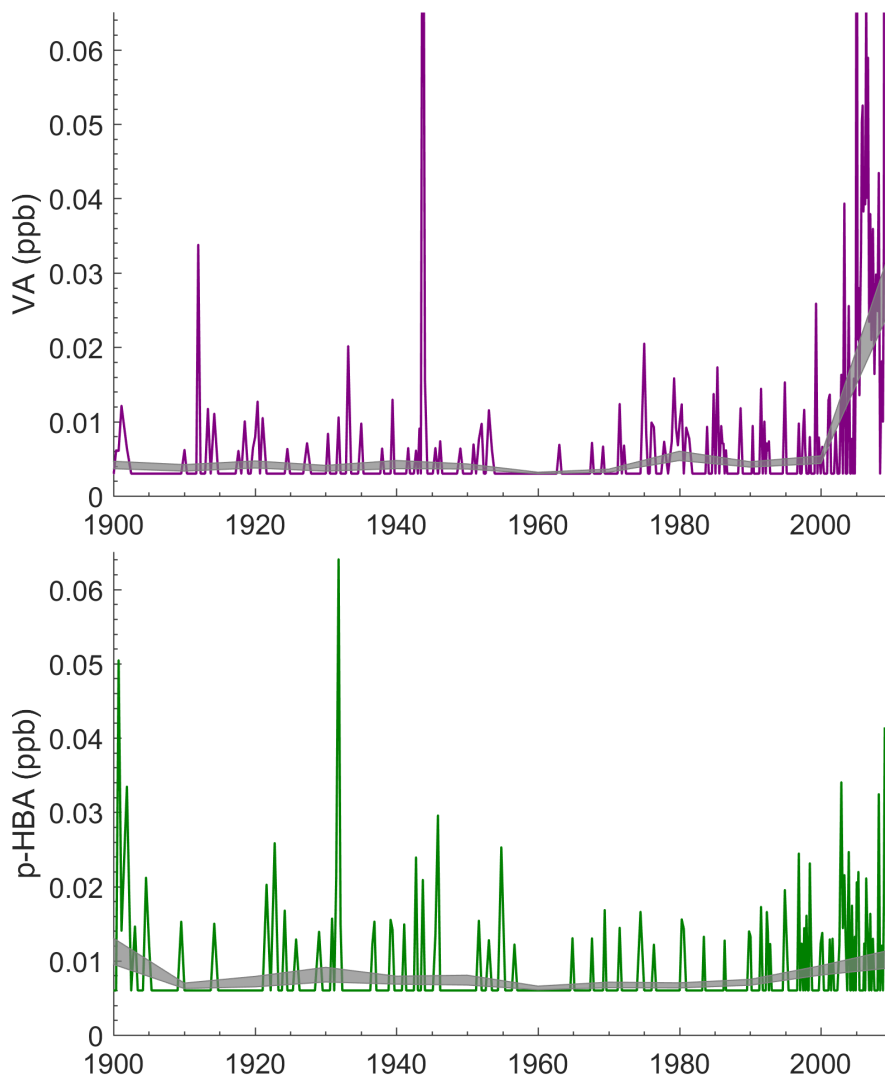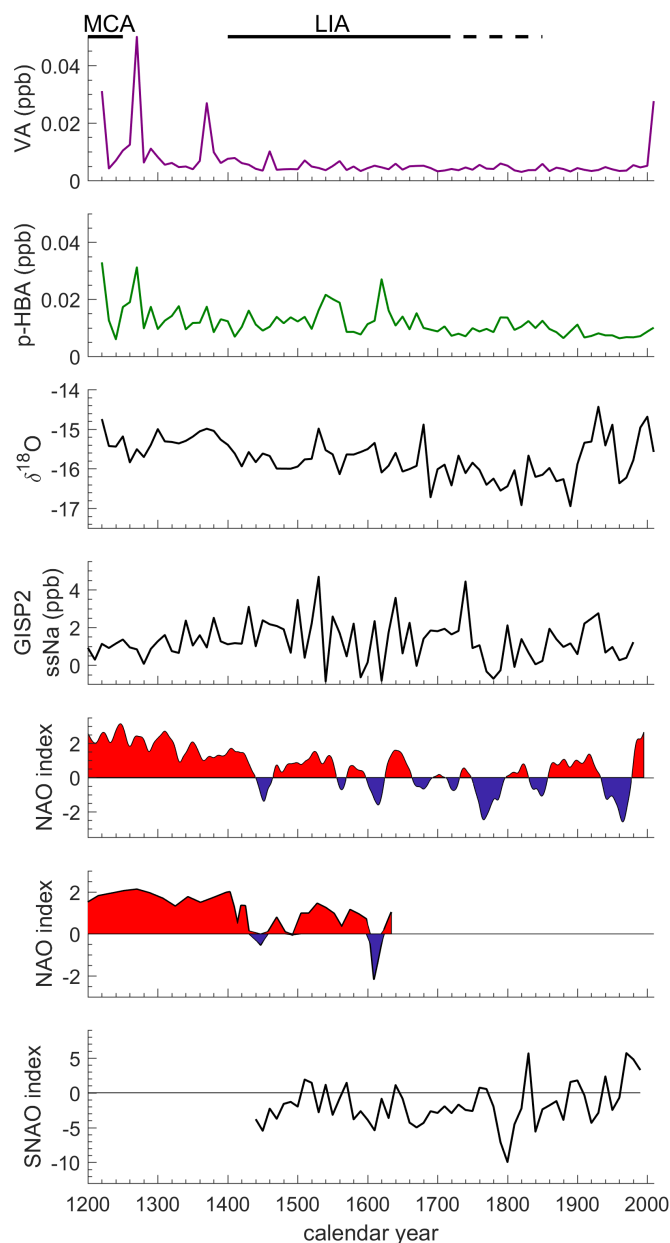
Figure 4. Lomonosovfonna ice core records of vanillic acid (top) and p-hydroxybenzoic acid (bottom) for the 20th century. Gray shaded areas are 10-year bin averages with ±1 standard error.

Figure 5. Aromatic acids in the Lomonosovfonna, Svalbard and Akademii Nauk ice cores. Left: vanillic acid, Right: p-hydroxybenzoic acid. Black lines are 10-year bin averages of the the Lomonosovfonna ice core measurements. Grey lines are the 10-year bin averages of the Akademii Nauk ice core measurements (Grieman et al., 2017). The black horizontal lines are the Medieval Climate Anomaly (MCA) and the Little Ice Age (LIA) (Mann et al., 2009). The dashed horizontal line is the extended LIA in the Svalbard region (Divine et al., 2011).
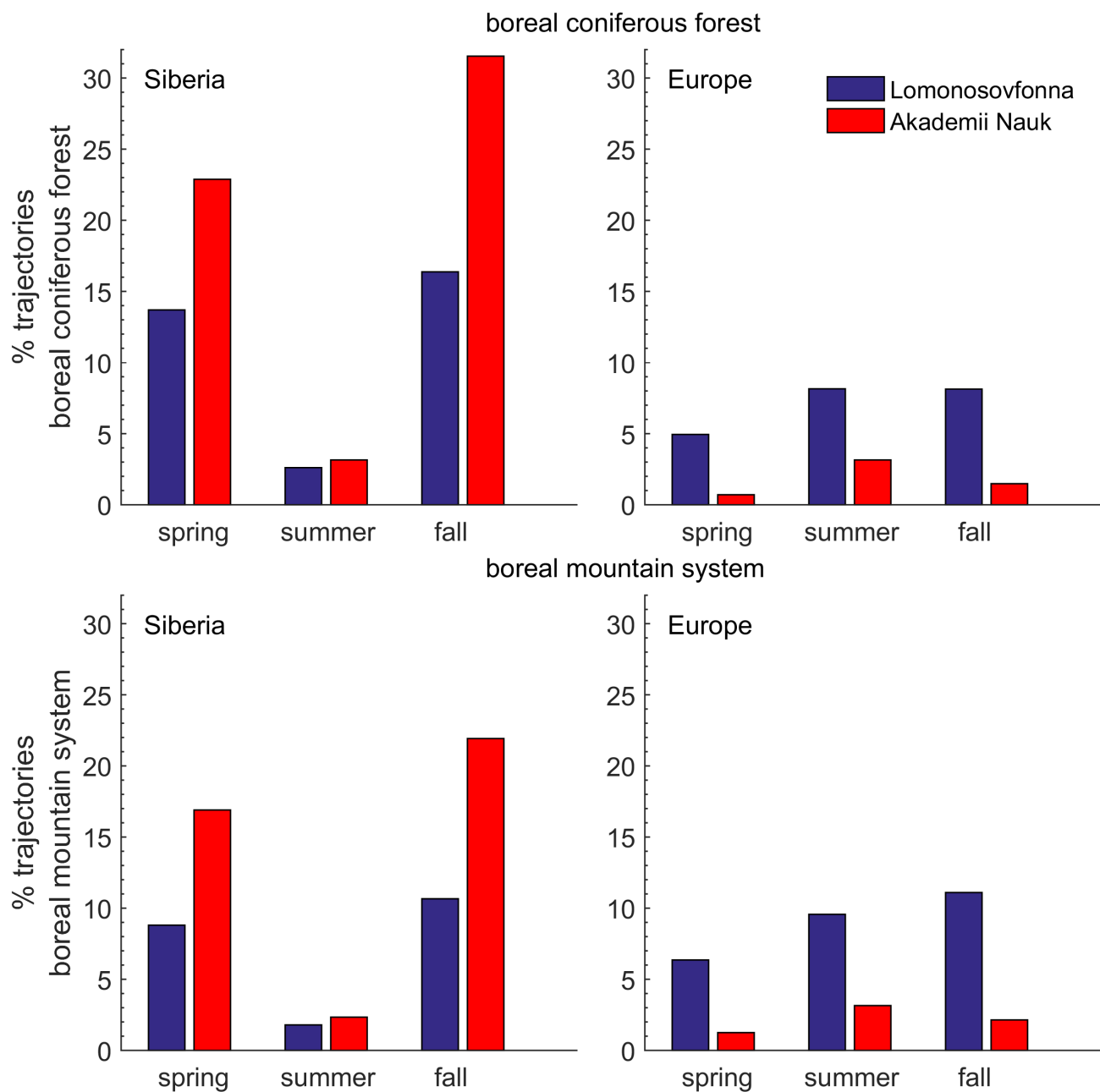
Figure 6. Back trajectories reaching the boreal ecosystems starting from the Lomonosovfonna and Akademii Nauk ice core locations. Blue is Lomonosovfonna. Red is Akademii Nauk. Trajectories reaching: Siberia (left), Europe (right), boreal coniferous forest (top), and boreal mountain system (bottom).

Figure 7. Comparison of the timing of aromatic acid signals in the Lomonosovfonna ice core over the past 800 years compared to other climate-related proxy records. From top: 10-year bin averages of Lomonosovfonna vanillic acid and p-hydroxybenxoic acid; 10-year bin averages of the oxygen isotope record from the Lomonosovfonna ice core (Wendl et al., 2015); 10-year bin averages of the GISP2 ice core D seasalt sodium (lower values correspond to positive NAO; Mayewski et al., 1997); North Atlantic Oscillation (NAO) index (red > 0; blue < 0; Trouet et al., 2009); NAO index (Olsen et al., 2012) (red > 0; blue < 0); and 10-year bin averages of the summer North Atlantic Oscillation (SNAO) index (Linderholm et al., 2009). The black horizontal lines are the timing of the Medieval Climate Anomaly (MCA) and the Little Ice Age (LIA) (Mann et al., 2009). The dashed horizontal line is the extended LIA in the Svalbard region (Divine et al., 2011).
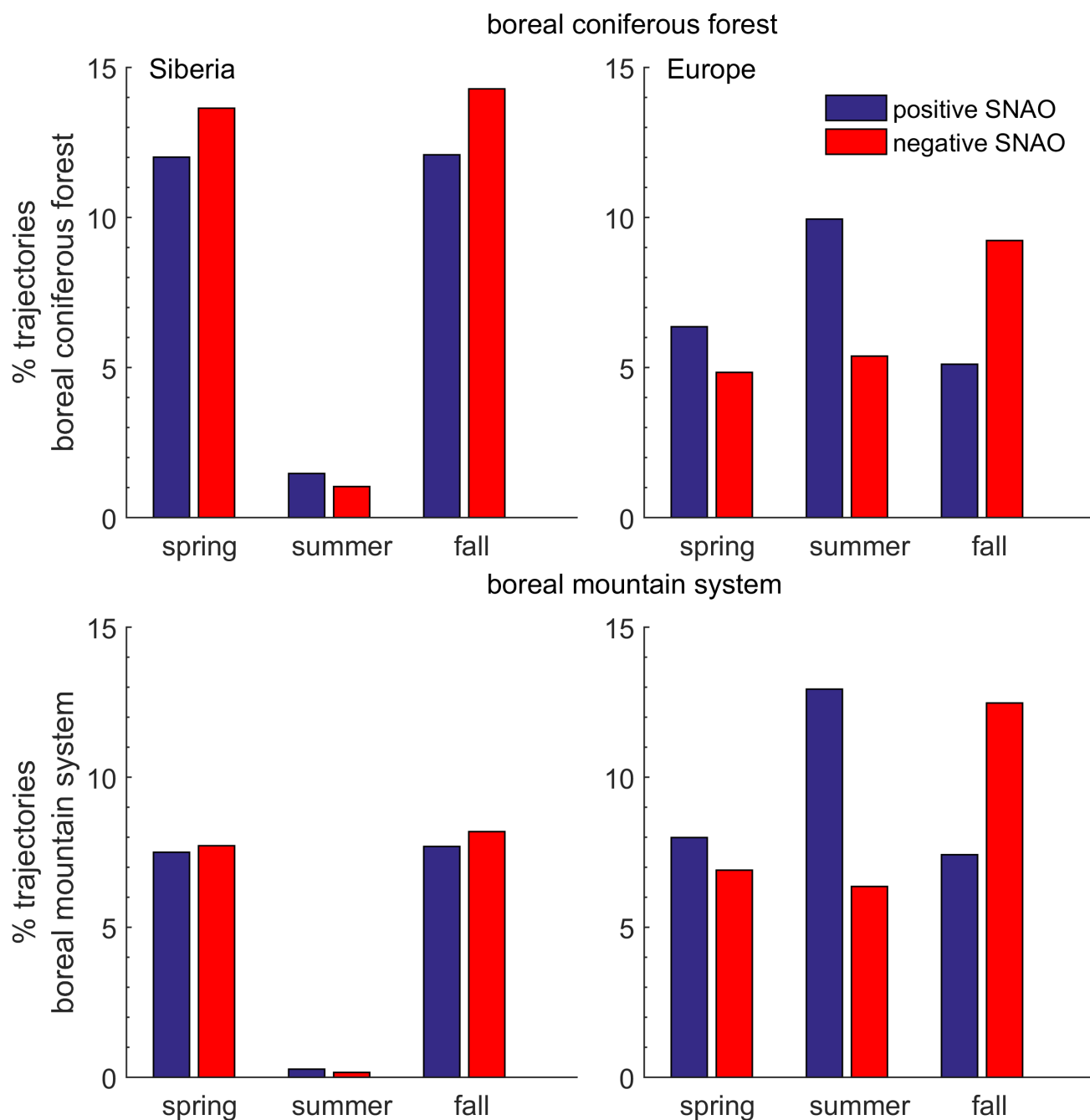
Figure 8. Back trajectories reaching the boreal ecosystems starting from the Lomonosovfonna ice core location. Blue is a positive SNAO pe-riod (1970-1979 CE). Red is a negative SNAO period (1948-1957 CE). Trajectories reaching: Siberia (left), Europe (right), boreal coniferous forest (top), and boreal mountain system (bottom).